Dye adsorbates BrPDI, BrGly, and BrAsp on anatase TiO_2(001) for dye-sensitized solar cell applications

D. Çakır,[1] O. Gülseren,[1,*] E. Mete,[2] and Ş. Ellialtıoğlu[3]
[1]*Department of Physics, Bilkent University, Ankara 06800, Turkey*
[2]*Department of Physics, Balıkesir University, Balikesir 10145, Turkey*
[3]*Department of Physics, Middle East Technical University, Ankara 06531, Turkey*
(Received 12 March 2009; revised manuscript received 1 July 2009; published 28 July 2009)

Using the first-principles plane-wave pseudopotential method within density functional theory, we systematically investigated the interaction of perylenediimide (PDI)-based dye compounds (BrPDI, BrGly, and BrAsp) with both unreconstructed (UR) and reconstructed (RC) anatase TiO_2(001) surfaces. All dye molecules form strong chemical bonds with surface in the most favorable adsorption structures. In UR-BrGly, RC-BrGly, and RC-BrAsp cases, we have observed that highest occupied molecular orbital and lowest unoccupied molecular orbital levels of molecules appear within band gap and conduction-band region, respectively. Moreover, we have obtained a gap narrowing upon adsorption of BrPDI on the RC surface. Because of the reduction in effective band gap of surface-dye system and possibly achieving the visible-light activity, these results are valuable for photovoltaic and photocatalytic applications. We have also considered the effects of hydration of surface to the binding of BrPDI. It has been found that the binding energy drops significantly for the completely hydrated surfaces.

DOI: 10.1103/PhysRevB.80.035431 PACS number(s): 73.20.Hb, 84.60.Jt, 68.43.Bc, 71.15.Mb

I. INTRODUCTION

The research on renewable energy sources is of greater importance than ever because of the increasing atmospheric carbon dioxide level as a result of the consumption of fossil fuels and growing demand on energy. Among them, solar cells are the photovoltaic devices in which light are converted to electricity. Although, silicon based solar cells are capable of stable and efficient solar energy conversion, their fabrication is expensive. Therefore, several studies has been conducted to develop less expensive although efficient alternatives. Dye-sensitized solar cells (DSSCs) (Refs. 1 and 2) have been a focus of attention because of their potential low cost and relatively high power conversion efficiency. There is a great deal of effort in order to improve the efficiency of DSSC by investigating various alternative dyes and semiconductor systems including surfaces, nanoparticles, nanotubes, and nanowires.[3–6] As a matter of fact, TiO_2 is widely used in DSSC as an active semiconductor metal oxide because it is chemically stable in different conditions, firm under illumination, non toxic, and relatively easy and cheap to produce. Moreover, in recent years, the titania anatase surfaces are studied from first-principles calculations for different properties and applications such as the microscopic mechanisms related to photogenerated electrons at titania-molecule interface[7] or the band-gap narrowing for enhanced photoelectrochemical activity.[8]

Even though among its polymorphs rutile structure is the most stable bulk phase for TiO_2, anatase phase is considered for the surfaces and nanocrystals since they are active and efficient for most of the applications based on these. Hence, the surface structures of anatase phase of titania are investigated in detail.[9–16,19] Most of anatase TiO2 crystal surfaces are dominated by the thermodynamically stable (101) surface which constitutes more than 94% of total exposed surface according to Wulff construction.[9] However, the minority (001) surface is much more reactive compared to (101) facet as also shown by density functional theory (DFT) calculations.[16] It was pointed out that (001) surface has an important role in observed properties such as reactivity of anatase nanoparticles, which cannot be explained by considering majority (101) surface. Relative stability of various low-index surfaces of anatase nanoparticles might be controlled by surface chemistry such as pH environment or hydroxilation, or particle size.[17,18] Another recent study showed that single-crystal anatase TiO_2 with a high percentage (001) surface can be synthesized by using hydrofluoric acid as a morphology controlling agent.[19] Furthermore, fluorated anatase surface can be easily cleaned to obtain fluorine free surface without altering the crystal structure and morphology. Because of the higher reactivity (which is crucial for promising solar cell applications) of the (001) surface compared to the (101) surface, we used (1×1) clean as well as (1×4) reconstructed (001) surfaces to study interaction between TiO_2 surface and adsorbate dye molecules.

In this study, we report the electronic properties of unreconstructed (UR) and reconstructed (RC) anatase TiO_2(001) surfaces with perylenediimide (PDI)-derived dye adsorbates, important for DSSC technology. We have obtained both adsorbate-induced occupied gap levels and band-gap narrowing. These results are essential for photovoltaic and photocatalytic applications. For these applications, adsorbate-surface system must be stable to illumination and physical and chemical processes that follow. Moreover, electronic structure of the whole system, including the surface and the adsorbed dye molecule, has ability to absorb a large part of the solar spectrum.

II. METHOD

We have performed first-principles plane-wave calculations[20,21] within DFT (Ref. 22) using projected

augmented-wave (PAW) potentials[23,24] with electronic configurations $3p^6 3d^3 4s^1$ for Ti and $2s^2 2p^4$ for O. The exchange-correlation contributions have been treated using generalized gradient approximation (GGA) with PW91 (Ref. 25) formulation. In this study, we have used slab geometry for surface calculations. The clean and (1×4) reconstructed anatase surfaces are modeled as a periodic slab with a four-layer thickness, which is enough to mimic anatase (001) surface.[9,13,16] It is very well known that surface properties of TiO_2 exhibit slow convergence, and the surface energy and the band gap show oscillations with the thickness of the surface slab.[14,26] Four-layer slab can be considered as the smallest representation of anatase (001). Since these large dye molecules have been considered with different surface coverages, the anatase (001) surface has been modeled by both periodic (2×4) (7.606 and 15.212 Å) and (4×4) (15.212 and 15.212 Å) surface unit cells (UR or RC) with four layers of slabs of TiO_2 containing at least 192 atoms; therefore, it is hard to use more thicker slab. We have imposed certain criteria for the choice of supercell dimensions. First of all, these supercells must be large enough to give possibility of searching different adsorption sites and of preventing the interaction of the dye molecules with its periodic images. Second, they must be thick enough to reasonably reproduce most of the TiO_2 bulk properties. The vacuum between the bottom of the slab and the top the adsorbed molecule has been taken at least 8 Å. In all calculations, only the atoms in the bottom surface have been fixed to their bulk truncated positions allowing all others to relax to their minimum-energy configurations by using conjugate gradient method where total energy and atomic forces are minimized. Maximum force magnitude that remained on each atom has been limited to 0.06 eV/Å. Isolated dye molecules have been relaxed in large orthorhombic supercells such that the spacing between the dye molecules has been taken as 8 Å in order to prevent interaction between adjacent isolated molecules. For Brillouin-zone integrations, in the self-consistent potential and total-energy calculations, Γ point and three special **k** points have been used for (4×4) and (2×4) supercells, respectively.[27] A plane-wave basis set with kinetic-energy cutoff of 500 eV has been used.

III. RESULTS AND DISCUSSIONS

The minimum-energy structures of UR and RC anatase TiO_2(001) surfaces are shown in Fig. 1. The coordination in bulk anatase is sixfold and threefold for Ti's and O's, respectively. However, the UR surface has twofold and threefold coordinated O and fivefold coordinated Ti atoms, while we have also fourfold Ti's in the case of the RC structure. Existence of undercoordinated atoms influences the chemical and physical properties of surfaces. In the relaxed structure of UR surface, we have inequivalent bridge O-Ti bonds with lengths of 2.21 and 1.76 Å for O1-Ti1 and O1-Ti2, respectively. Ti1-O1-Ti2 bond angle is 146.3°. (1×1) anatase (001) surface is not very stable. However, it can be stabilized upon hydration or reconstruction of surface attained by heating to elevated temperatures.[12] For the RC surface case, we have considered the reconstruction model proposed by

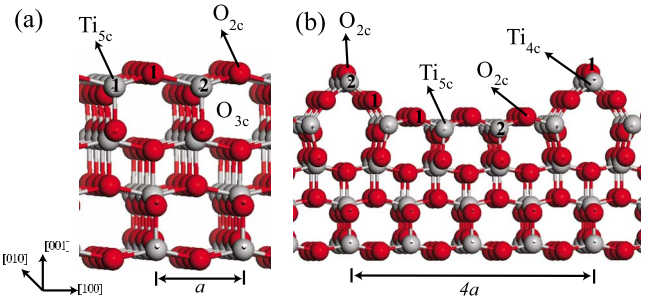

FIG. 1. (Color online) Side views of the minimum-energy geometries of (a) UR and (b) RC surfaces having (1×1) and (1×4) periodicities, respectively, where a (=3.803 Å) is the theoretical bulk lattice constant. The coordinations of some of the atoms are indicated as subscripts.

Lazzeri and Selloni[13] named ad-molecule (ADM) model. According to this model, stress of surface is released upon reconstruction. Strong asymmetric bridge O-Ti bond lengths disappear and resulting Ti1-O1 bridge bond lengths range from 1.79 to 1.98 Å. We have calculated the surface energy (E_T[surface]) of UR and RC surfaces through the following formula: $E_T[\text{surface}]=(E_T[\text{slab}]-E_T[\text{bulk}])/(\text{total exposed area})$. E_T[slab] and E_T[bulk] are the total energies of the slab and the bulk anatase containing equal number of TiO_2 units with the slab. The calculated E_T[surface] is 0.122 and 0.087 eV/Å^2 for UR and RC structures, respectively. We noticed that UR surface is energetically less stable compared to RC.

Optimized molecular structures of PDI-based brominated dye compounds are shown in Fig. 2, in which carboxyl groups, namely, glycine (Gly) and aspartine (Asp) groups, are asymmetrically attached to the tips in the cases of BrGly and BrAsp, respectively. These molecules can be excited under visible-light illumination without undergoing molecular deformation. Time-dependent density functional theory (TD-

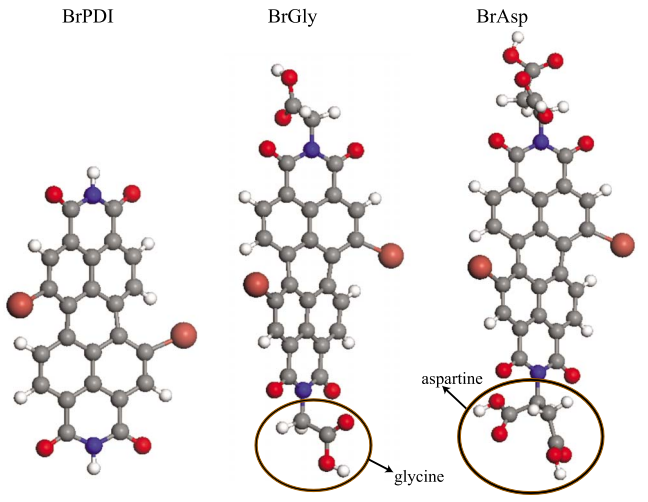

FIG. 2. (Color online) Relaxed molecular structures of PDI-based dye molecules. Large gray (pink), white (white), small gray (gray), dark (red), and dark at the corner of hexagons (blue) balls represent the Br, H, C, O, and N atoms, respectively. Carboxyl groups are also shown.

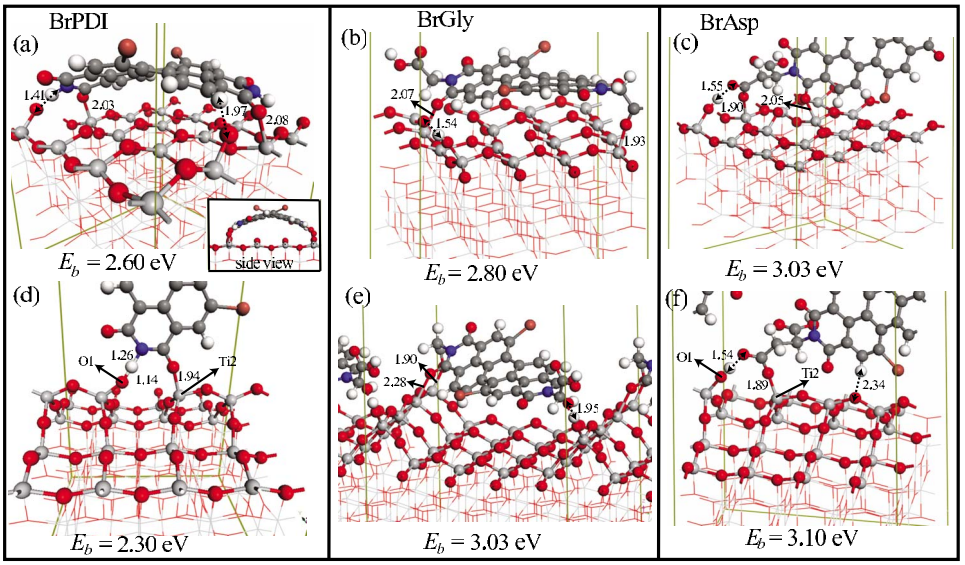

FIG. 3. (Color online) Fully optimized geometry of the most energetically stable adsorption modes of dye molecules on anatase TiO_2(001) surfaces. Inset shows the side perspective structure viewed from [100] direction of UR-BrPDI case. Only the bonded part of molecules is represented. Detailed structure of dyes is shown in Fig. 2. Binding energies and interatomic distances (in Å) between the selected atoms are also indicated. Discussions about the labeled atoms are given in the text.

DFT) corrected highest occupied molecular orbital– lowest unoccupied molecular orbital (HOMO-LUMO) gaps for these organic dyes fall within the visible region with values 2.39, 2.38, and 2.36 eV for BrPDI, BrGly, and BrAsp, respectively; while the corresponding DFT results are all 1.45 eV. Therefore, they can be considered as potential candidates in DSSC applications, which absorb photons to generate electron-hole pairs. Detailed discussions about these dye molecules have been published elsewhere.[28]

We have considered several probable adsorption configurations for each of the dyes to find the most favorable binding geometry. In Fig. 3, we have presented the most energetically stable adsorption structures. Binding energy E_b of molecules has been calculated by the following expression, $E_b = E_T[\text{slab}] + E_T[\text{dye}] - E_T[\text{slab+dye}]$ in terms of the total energy of clean slab, dye molecule, and optimized slab +dye system. Our calculations suggest significant binding characteristics for these dye-surface systems. In all strong chemisorption modes, dye molecules tend to bind to the undercoordinated Ti ions on the surface via its O atoms. Hydrogen atoms, on the other hand, prefer to be bonded to the surface bridge O atoms. Strong binding between dyes and surfaces is very crucial for the performance and production of DSSCs.

BrPDI case: this dye molecule does not have any carboxyl groups. UR adsorption geometry, as seen in Fig. 3(a), has been driven by the two O atoms at each end binding to fivefold coordinated Ti atoms in the expense of induced stress on the bent dye molecule, which was initially almost parallel to the surface. Hence, the main contribution to E_b comes from these bonds. Due to interaction with H atoms, two bridge O atoms go upward, breaking two surface Ti-O bridge bonds. The resulting E_b of this adsorption mode is 2.30 eV. If one side of dye does not bind to surface, E_b reduces to 1.41 eV. Average distance between molecule O and surface Ti atoms is about 2.0 Å. In RC case, molecule prefers to bind the ridge atoms of the surface. Unlike Ti atoms on terrace region, the ones on the ridge are fourfold coordinated. Therefore, the ridge is more reactive than the terrace region. For example, in the case of surface wetting, it has been shown that molecular and dissociative water adsorptions occur on the terrace and ridge regions, respectively.[16,29] As shown in Fig. 3(d), hydrogen atoms of the dye bind to surface O1 atoms by breaking O1-Ti2 bonds on the RC surface. This is the strongest binding achieved for RC-BrPDI structure giving an E_b of 2.30 eV. Unlike UR-BrPDI case, mainly the structure of the surface at the proximity of the dye is disturbed in the RC case.

BrGly case: BrGly molecule has two glycine groups. The glycine ligand anchors BrGly to the titania as shown in Figs. 3(b) and 3(e). In the UR-BrGly structure, one of the ligand and perylene O atoms binds to surface Ti atoms. The remaining middle part of the dye is almost parallel to the surface. The other ligand does not bind to any surface atom. Average interatomic distance between the bonded surface Ti and dye O atoms is about 2 Å. This dye makes two contacts with the surface giving rise to increased interaction. Moreover, dye is dissociatively adsorbed throughout the UR surface. H atom of the bonded ligand part is captured by the surface bridge O atom. E_b of this adsorption mode is 2.80 eV, which is greater than E_b of BrPDI case on the same surface. In the RC case, E_b of the dye on this surface increases significantly being the strongest chemisorption mode achieved for BrGly dye-surface systems. Resulting binding energy is 3.03 eV. This corresponds to a dissociative adsorption in which ligand O-H bond breaks. This hydrogen binds to the surface ridge O atom becoming separated from the glycine O by 1.95 Å. Both ends of the dye interact with the ridge part of the RC surface. Being more energetic than the molecular adsorption, this result suggests that better anchoring leads to relatively higher E_b and stability.

BrAsp case: this dye contains two aspartine molecules as carboxyl groups. In the structure of aspartine, two O atoms are only onefold coordinated. At least, one of these oxygens participates in all strong binding modes. BrAsp exhibits dissociative binding on both surfaces as shown in Figs. 3(c) and 3(f). One of the aspartine O-H bonds breaks, and this H atom binds to surface O1 atom as in the case of RC-BrGly structure. The dye molecule sticks to UR surface Ti atoms through its aspartine oxygens giving a binding energy of 3.03

eV. In RC case, onefold coordinated O atom of the ligand part of the dye binds to fourfold coordinated Ti atom, which is in the ridge region on the surface. Existence of this catalytically active region, similar to RC-BrGly case, allows BrAsp to form strong chemical bonds with the RC surface leading to an E_b of 3.10 eV. We also notice that the coordination numbers of ligand O atoms and surface Ti atoms influence the strength of the binding.

We did also study the effects of coverage on E_b for BrPDI adsorption on both (2×4) UR and RC surfaces. Because of the size of these slabs, only some adsorption modes have been investigated. High coverage reduces the E_b significantly. When BrPDI binds to diagonal Ti atoms through its two O atoms, E_b is 1.60 eV on (4×4) cell. However, on (2×4) slab, E_b becomes 0.87 eV. Stability of (001) anatase can be enhanced not only with reconstruction but also via adsorption of water. Thus, we have studied the interaction of BrPDI with these surfaces where water has been adsorbed dissociatively. In RC surface, water adsorption occurs only at ridge region. Direct interaction between BrPDI and the host surface is prevented by the water. In addition to this, reactivity of surface reduces due to the adsorption of water. Therefore, E_b drops compared to the clean surface and binding mainly comes from the interaction between surface hydroxyl groups and the dye molecule.

In DSSC devices, optical properties of the systems are determined by the dye molecules. To produce an efficient and stable solar cell, dye molecules must be strongly bound to the underlying semiconductor material and absorb the large part of the solar light. Our dyes are stable at their ground state and form strong chemisorption bonds with the TiO_2 surface. Except the UR-BrPDI case, structure of the studied dye molecules is slightly changed upon adsorption only at the proximity of binding region. We have further investigated the electronic properties of fully relaxed surface+dye combined system. In DSSC, dye is excited by photons and as a result electron-hole pairs are generated by this illumination. Generated electrons in excited states of dye must be injected to conduction band of semiconductor, and this injection has to be very fast to prevent the reduction in the oxidized dye. Therefore, position of HOMO-LUMO levels of the dyes with respect to valence-band (VB) and conduction-band (CB) edges of TiO_2 is very crucial. For an efficient solar cell, HOMO level produces occupied levels inside the gap region and LUMO is well localized across CB of the slab. Figure 4 shows the PDOS of the surface+dye systems for the most energetically stable adsorption modes. We notice that adsorbed BrGly's on both surfaces and BrAsp on the RC surface induce occupied states inside the band gap of TiO_2. Moreover, LUMO levels of these molecules fall inside the CB of the slab. In RC-BrPDI, HOMO and LUMO levels of the dyes appear as edges of VB and CB of the oxide, respectively. As opposed to the UR-BrPDI case, the adsorption of BrPDI induces significant band-gap narrowing. Due to coupling between the electronic states of the dyes and anatase surfaces, there are both broadening and shift to higher energies in the energy levels of the dye molecules. The effects of these strong interactions are more pronounced in the occupied levels of the dyes. Yet, HOMO-LUMO gaps do not change significantly. Therefore, these molecules do not lose their optical properties, which are vital for DSSC applications.

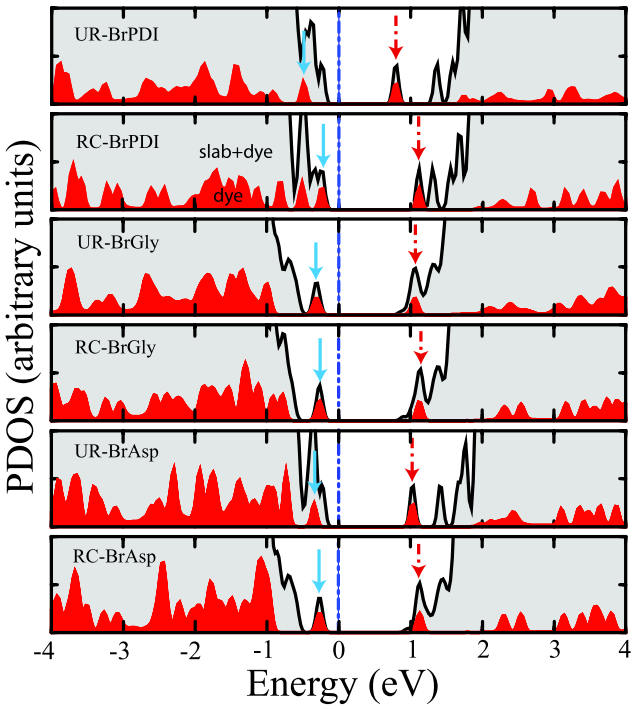

FIG. 4. (Color online) Partial densities of states (PDOS) for the adsorbed dyes. DOS of total system and adsorbed dye are represented by gray and red colors, respectively. Fermi level is shown by the violet dotted-dashed line. Cyan and dotted-dashed red arrows mark the positions of HOMO and LUMO levels of the adsorbed dye molecules.

Electronic structure calculations show that the adsorption of dye molecules may result in a redshifted spectrum for the titania surface due to band-gap narrowing by suitable positioning of the HOMO and LUMO levels relative to the oxide band edges. This might lead to visible-light absorption in the DSSC application. However, strong absorption at these lower energies is possible if only the transitions are symmetry allowed. For this reason we have evaluated the dipole matrix elements between occupied and empty states for each case. The calculated absorption spectra[30] for clean anatase surface and the isolated dye molecules are depicted along with those for the corresponding dye-surface composite systems in Fig. 5. The calculated $\varepsilon_2(\omega)$ for the reconstructed surface systems are shown in the upper panel, whereas those for the unreconstructed surface are presented in the lower panel, and the corresponding curves for the isolated dyes are given as inverted in the lower panel. For both of the clean surfaces, clean RC and UR (black solid curve), absorption starts after about 2 eV consistent with the calculated band gaps. Similarly, isolated molecules show first strong absorption around 1.4 eV reflecting their calculated HOMO-LUMO gaps.[28] For the composite systems on both type of surfaces, first strong absorption peak arises at energies slightly lower than 1.4 eV and the second peak around 2.3 eV. Comparison of these to the spectra of isolated dye molecules and clean surfaces indicates that the first peak is slightly redshifted first peak of the dye molecule, while the second peaks coincide with the

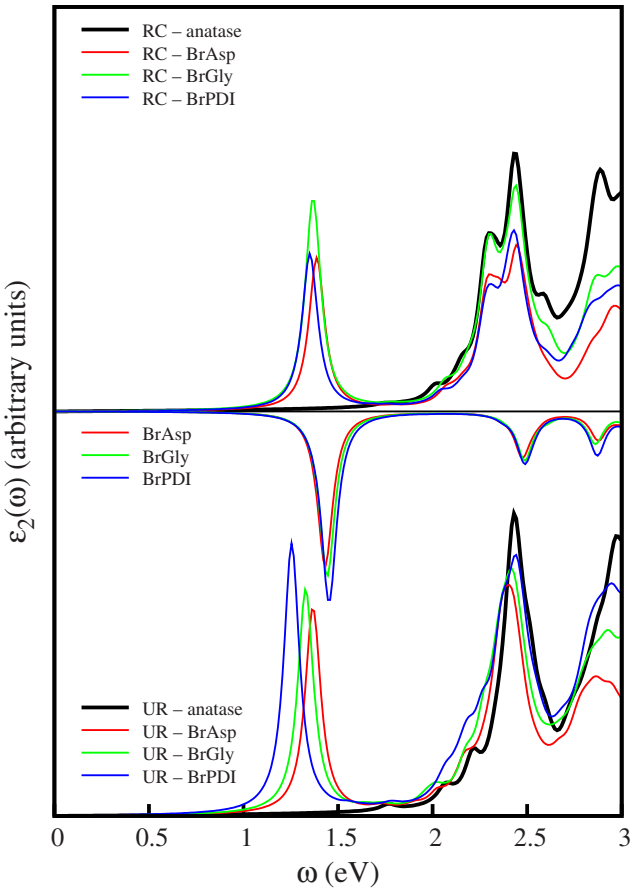

FIG. 5. (Color online) Absorption spectra of isolated dye molecules (inverted in lower panel), those of adsorbed dye on unreconstructed (lower panel), and reconstructed (upper panel) anatase surfaces compared also with the clean surface for both surfaces (black solid curves).

first peaks of the clean surfaces. Hence, one can conclude that the first peak mainly contributed by the transitions from the states due to dye-HOMO levels appeared within the band gap around the valence-band top to the conduction-band-edge states and/or to the LUMO levels of the dye near CB minimum. Therefore, these transitions are dipole allowed and are suitable for DSSC applications. However, one needs to note that for the precise description of the excited states it is necessary to go beyond this static DFT calculations, e.g., TDDFT. The TDDFT with proper charge-transfer excitations treatment[31] of dye+surface systems would give more accurate results, yet it is computationally demanding. The comparison between the DFT and the TDDFT results for the energy levels of these dye molecules in Ref. 28 suggests a rigid shift of the first (dye originated) absorption peak to higher in energies within the visible region.

Strong dye-surface interaction influences the ultrafast electron transfer from the excited state of the molecule to an unoccupied conduction band of TiO_2. Strong interaction means delocalization of dye LUMO level over the whole system. Transfer rate of electrons can be obtained from the electronic structure calculations by using the Newns-Anderson model.[32] Due to coupling between dye and surface electronic states, a particular molecular energy level (E_M) of the adsorbed dye molecule is broadened into a resonance centered around ε and has a Lorentzian shape with a width of Γ. By calculating the full width at half maximum of the LUMO level, which gives the lifetime broadening $\hbar\Gamma$, one obtains the ultrafast electron injection time τ through $\tau = \hbar/\hbar\Gamma$ or $\tau(\text{fs}) = 658/\hbar\Gamma(\text{meV})$.[33]

IV. CONCLUSIONS

In conclusion, adsorption of BrPDI, BrGly, and BrAsp dye molecules on UR and RC anatase $TiO_2(001)$ surfaces adapts the electronic structure of combined system and lowers the optical threshold to visible light. Resulting electronic structure depends on the type of the dye molecule as well as the surface structure. BrPDI causes gap narrowing when it is adsorbed by the RC surface. In UR-BrGly, RC-BrGly, and RC-BrAsp dye-surface systems, HOMO level of molecule appears in the band-gap region. We have shown that these molecules form strong chemical bonds with both of the UR and RC surfaces. Therefore, surface+dye system is very stable. Our results are fundamental and useful for applications in the area of photovoltaics and photocatalysis.

ACKNOWLEDGMENTS

We acknowledge the State Planning Office DPT, UNAM National Nanotechnology Center Project computational facilities and METU YUUP projects. Part of the calculations has been carried out at ULAKBIM Computer Center and UYBHM at Istanbul Technical University. E.M. and S.E. acknowledge the partial support by TÜBİTAK (Project No. 107T560), and O.G. acknowledges the support of Turkish Academy of Sciences, TÜBA.

*gulseren@fen.bilkent.edu.tr

[1] B. O'Regan and M. Grätzel, Nature (London) **353**, 737 (1991).
[2] M. Grätzel, Nature (London) **414**, 338 (2001).
[3] F. De Angelis, S. Fantacci, A. Selloni, M. Grätzel, and M. K. Nazeeruddin, Nano Lett. **7**, 3189 (2007).
[4] F. De Angelis, S. Fantacci, A. Selloni, M. K. Nazeeruddin, and M. Grätzel, J. Am. Chem. Soc. **129**, 14156 (2007).
[5] D. P. Hagberg, J.-H. Yum, H. Lee, F. De Angelis, T. Marinado, K. M. Karlsson, R. Humphry-Baker, L. Sun, A. Hagfeldt, M. Grätzel, and M. K. Nazeeruddin, J. Am. Chem. Soc. **130**, 6259 (2008).
[6] S. Meng, J. Ren, and E. Kaxiras, Nano Lett. **8**, 3266 (2008).
[7] M.-H. Du, J. Feng, and S. B. Zhang, Phys. Rev. Lett. **98**, 066102 (2007).
[8] Y. Gai, J. Li, S.-S. Li, J.-B. Xia, and S.-H. Wei, Phys. Rev. Lett. **102**, 036402 (2009).

[9] M. Lazzeri, A. Vittadini, and A. Selloni, Phys. Rev. B **63**, 155409 (2001).
[10] A. Beltran, J. R. Sambrano, M. Calatayud, F. R. Sensato, and J. Andres, Surf. Sci. **490**, 116 (2001).
[11] M. Calatayud and C. Minot, Surf. Sci. **552**, 169 (2004).
[12] G. S. Herman and M. R. Sievers, Phys. Rev. Lett. **84**, 3354 (2000).
[13] M. Lazzeri and A. Selloni, Phys. Rev. Lett. **87**, 266105 (2001).
[14] F. Labat, P. Baranek, and C. Adamo, J. Chem. Theory Comput. **4**, 341 (2008).
[15] A. Vittadini, M. Casarin, and A. Selloni, Theor. Chem. Acc. **117**, 663 (2007).
[16] X.-Q. Gong and A. Selloni, J. Phys. Chem. B **109**, 19560 (2005).
[17] A. S. Barnard and L. A. Curtiss, Nano Lett. **5**, 1261 (2005).
[18] A. Feldhoff, C. Mendive, T. Bredow, and D. Bahnemann, ChemPhysChem **8**, 805 (2007).
[19] H. G. Yang, C. H. Sun, S. Z. Qiao, J. Zou, G. Liu, S. C. Smith, H. M. Cheng, and G. Q. Lu, Nature (London) **453**, 638 (2008).
[20] M. C. Payne, M. P. Teter, D. C. Allen, T. A. Arias, and J. D. Joannopoulos, Rev. Mod. Phys. **64**, 1045 (1992).
[21] Computations have been carried out with the VASP software: G. Kresse and J. Hafner, Phys. Rev. B **47**, 558 (1993); G. Kresse and J. Furthmüller, *ibid.* **54**, 11169 (1996).
[22] W. Kohn and L. J. Sham, Phys. Rev. **140**, A1133 (1965); P. Hohenberg and W. Kohn, *ibid.* **136**, B864 (1964).
[23] P. E. Blöchl, Phys. Rev. B **50**, 17953 (1994).
[24] G. Kresse and D. Joubert, Phys. Rev. B **59**, 1758 (1999).
[25] J. P. Perdew, J. A. Chevary, S. H. Vosko, K. A. Jackson, M. R. Pederson, D. J. Singh, and C. Fiolhais, Phys. Rev. B **46**, 6671 (1992).
[26] A. Vittadini and M. Casarin, Theor. Chem. Acc. **120**, 551 (2008).
[27] H. J. Monkhorst and J. D. Pack, Phys. Rev. B **13**, 5188 (1976).
[28] E. Mete, D. Uner, M. Çakmak, O. Gulseren, and Ş. Ellialtıoğlu, J. Phys. Chem. C **111**, 7539 (2007).
[29] X.-Q. Gong, A. Selloni, and A. Vittadini, J. Phys. Chem. B **110**, 2804 (2006).
[30] K. M. Glassford and J. R. Chelikowsky, Phys. Rev. B **45**, 3874 (1992).
[31] M. J. G. Peach, P. Benfield, T. Helgaker, and D. J. Tozer, J. Chem. Phys. **128**, 044118 (2008).
[32] D. M. Newns, Phys. Rev. **178**, 1123 (1969); N. A. Anderson and T. Lian, Annu. Rev. Phys. Chem. **56**, 491 (2005).
[33] P. Persson, M. J. Lundqvist, R. Ernstorfer, W. A. Goddard III, and F. Willig, J. Chem. Theory Comput. **2**, 441 (2006).